

## Article

# Flexible Potentiometric Sensor System for Non-Invasive Determination of Antioxidant Activity of Human Skin: Application for Evaluating the Effectiveness of Phytocosmetic Products

Aleksy V. Tarasov , Ekaterina I. Khamzina, Maria A. Bukharinova and Natalia Yu. Stozhko \* 

Scientific and Innovation Center of Sensor Technologies, Department of Physics and Chemistry, Ural State University of Economics, 8 Marta St., 62, 620144 Yekaterinburg, Russia; tarasov\_a.v@bk.ru (A.V.T.); xei260296@mail.ru (E.I.K.); mbuharinova@mail.ru (M.A.B.)

\* Correspondence: sny@usue.ru; Tel.: +7-343-283-1013

**Abstract:** In contemporary bioanalysis, monitoring the antioxidant activity (AOA) of the human skin is used to assess stresses, nutrition, cosmetics, and certain skin diseases. Non-invasive methods for skin AOA monitoring have certain advantages over invasive methods, namely cost-effectiveness, lower labor intensity, reduced risk of infection, and obtaining results in the real-time mode. This study presents a new flexible potentiometric sensor system (FPSS) for non-invasive determination of the human skin AOA, which is based on flexible film electrodes (FFEs) and membrane containing a mediator ( $[\text{Fe}(\text{CN})_6]^{3-/4-}$ ). Low-cost available materials and scalable technologies were used for FFEs manufacturing. The indicator FFE was fabricated based on polyethylene terephthalate (PET) film and carbon veil (CV) by single-sided hot lamination. The reference FFE was fabricated based on PET film and silver paint by using screen printing, which was followed by the electrodeposition of precipitate containing a mixture of silver chloride and silver ferricyanide (SCSF). The three-electrode configuration of the FPSS, including two indicator FFEs (CV/PET) and one reference FFE (SCSF/Ag/PET), has been successfully used for measuring the skin AOA and evaluating the impact of phytocosmetic products. FPSS provides reproducible ( $\text{RSD} \leq 7\%$ ) and accurate (recovery of antioxidants is almost 100%) results, which allows forecasting its broad applicability in human skin AOA monitoring as well as for evaluating the effectiveness of topically and orally applied antioxidants.



**Citation:** Tarasov, A.V.; Khamzina, E.I.; Bukharinova, M.A.; Stozhko, N.Y. Flexible Potentiometric Sensor System for Non-Invasive Determination of Antioxidant Activity of Human Skin: Application for Evaluating the Effectiveness of Phytocosmetic Products. *Chemosensors* **2021**, *9*, 76. <https://doi.org/10.3390/chemosensors9040076>

Academic Editor: Maria Luz Rodriguez-Mendez

Received: 9 March 2021

Accepted: 6 April 2021

Published: 9 April 2021

**Publisher's Note:** MDPI stays neutral with regard to jurisdictional claims in published maps and institutional affiliations.



**Copyright:** © 2021 by the authors. Licensee MDPI, Basel, Switzerland. This article is an open access article distributed under the terms and conditions of the Creative Commons Attribution (CC BY) license (<https://creativecommons.org/licenses/by/4.0/>).

**Keywords:** contact hybrid potentiometric method; human skin; antioxidant activity; carbon veil; flexible film electrode; phytocosmetics

## 1. Introduction

The skin is the largest organ of the human body and performs several vital functions, such as protective, sensory, thermoregulatory and others. Similar to any other organ, the skin is exposed to reactive species (RS), which may exist as radicals and non-radicals [1,2]. In physiological concentrations, RS impact cellular metabolism processes, such as protection against infectious pathogens, intracellular and intercellular signaling, redox regulation, and they are neutralized by antioxidants [1–3]. Various environmental factors (e.g., radiations, pollutants) and physiological factors, such as unhealthy lifestyle or unbalanced exercise, lead to RS overproduction and may change the redox homeostasis of the skin [1,2,4]. In pathological (elevated) concentrations, RS can cause irreversible changes in cellular compartments, inflammation, weakening of immune functions, and tissue degradation [1,2]. In addition, current research shows a link between high levels of RS, aging [1,2,5], and skin diseases [1,2,6]. The use of antioxidants in topical cosmeceuticals and oral nutraceuticals aims to achieve and maintain the redox balance of the skin [2,7]. For this reason, methods and sensors that measure the antioxidant status of the skin have

great potential for the use in cosmetics and food industries. In recent years, the cosmetics industry has focused on the use of biologically active plant-based ingredients with a reliable safety profile, which have evolved as “phytocosmetics” [8].

In the literature, there is still a lack of unified terminology to characterize the antioxidant status of a test sample. The most popular are “antioxidant activity”, “antioxidant capacity”, the total content of antioxidant compounds of a certain class and other terms [9]. In this paper, we will be using the term “antioxidant activity” (AOA), which is related to the concept of effective concentration of a substance accepted in chemistry. Effective concentration (activity) is a parameter of the Nernst equation used in potentiometry and in this work.

The methods used to measure the skin AOA can be classified into invasive, semi-invasive, and non-invasive according to the method of obtaining samples [10]. Invasive methods are based on obtaining skin specimens of certain thickness (epidermis and dermis) [11,12] or suction blister fluid from the epidermis [13], which is possible only in clinical settings with the involvement of medical staff. Semi-invasive methods are based on the use of an adhesive tape that collects the cells of the stratum corneum (corneocytes) [14]. The skin samples obtained by these methods require the extraction of antioxidants. Skin extracts are usually analyzed using high-performance liquid chromatography and spectrophotometric methods. The shortcomings of invasive and semi-invasive methods are that these methods are labor-intensive, uneconomical, and impractical to use in studies involving a large number of test subjects (screening).

Non-invasive methods are based on performing measurements directly on a testable skin area in real time and include reflection [15–17], resonance Raman [16–19], and electron paramagnetic resonance spectroscopy [19–21]; linear sweep [22] and cyclic [23,24] voltammetry; and potentiometry [25–30]. Non-invasive methods enable study of the impact of stresses, nutrition, cosmetics, and diseases on the skin AOA in vivo. The studies have reported correlations between reflection and resonance Raman spectroscopy [16,17] as well as resonance Raman and electron paramagnetic resonance spectroscopy [19]. However, reflection and resonance Raman spectroscopy have limitations, since they are able to measure only one class of skin antioxidants (carotenoids). In addition, resonance Raman spectroscopy presents an advantage in terms of measurement accuracy, but it uses more expensive apparatus compared with reflection spectroscopy. Electron paramagnetic resonance spectroscopy requires more complex instruments and, consequently, more qualified staff to operate them, which adds complexity to using this method for screening. With linear sweep and cyclic voltammetry, the results depend on the active area of the working electrode that can vary from electrode to electrode and may affect the value and reproducibility of the assay. In addition, these electrochemical methods differ by uncompensated charging current, which confines the detection limit value [31].

The simplest non-invasive method for monitoring the skin AOA is the potentiometric technique, which relies on using  $\text{Fe}^{3+/2+}$ -chelate [25] or  $[\text{Fe}(\text{CN})_6]^{3-/4-}$  [26–30] mediators. The use of  $[\text{Fe}(\text{CN})_6]^{3-/4-}$  seems to be more efficient, as it reduces the measurement time from 30 to 10 min. This method variation was later called the contact hybrid potentiometric method (CHPM) [30] and could have two modifications: when  $[\text{Fe}(\text{CN})_6]^{3-/4-}$  was introduced into an electrically conductive gel [26–28] or in a polymer membrane [29,30]. The use of a polymer membrane has led to better reproducible measurement results due to the elimination of the problems caused by different thickness of the gel layer and uneven distribution of  $[\text{Fe}(\text{CN})_6]^{3-/4-}$  [29]. However, multiple uses of a commercially available platinum screen-printed electrode requires its sterilization (when changing a respondent) and regeneration (after taking a series of measurements), which can be performed during a single procedure of high-temperature annealing [32]. It is obvious that the application of a sensory system with disposable components is of a more practical value. Brainina et al. [30] proposed a single-use potentiometric sensor system to evaluate the AOA of human skin; however, the obtained results showed a lower degree of reproducibility as compared with a sensor system relying on a commercial platinum screen-printed electrode.

It is known that the reproducibility of tactile skin sensors is related to the following factors: effective sampling, i.e., transport of the analyte to the sensor surface [33]; sensor contamination [33,34]; skin condition variability [34]; and poor contact resulting in an unreliable analytical signal [35]. This paper adopts three strategies aimed at improving the result reproducibility when determining the human skin AOA by the CHPM. Following the first strategy, the proposed sensor system should be disposable, which eliminates its contamination during repeated use and makes it safe for a respondent. The second strategy focuses on the need to create a three-electrode sensor system configuration, which enables receiving two results during one measurement, thus eliminating a possible impact of time-varying skin conditions. The third strategy implies the use of flexible film electrodes (FFEs) as part of the sensor system, which ensures better contact at the heterogeneous "electrode/membrane with  $[\text{Fe}(\text{CN})_6]^{3-/4-}$ /skin" interface and contributes to the measurement of a stable analytical signal (potential) under load conditions (local pressure). Finally, a carbon veil (CV) was used for fabricating the indicator FFE. Since the CV displays such features as electrical conductivity, softness, and flexibility, it is these features that explain the CV popularity in applied electrochemistry. The CV can be used for manufacturing electrodes for batteries [36], capacitors [37], microbial fuel cells [38], and generator cells [39]; heating elements [40]; and sensors for the determination of ascorbic acid [41] and nitrite ions [42]. The analysis of Web of Science and Scopus publications has not revealed any case reporting the use of CV for monitoring the AOA of biological objects.

## 2. Materials and Methods

### 2.1. Chemicals

The following chemicals were used:  $\text{K}_3[\text{Fe}(\text{CN})_6]$ , KCl,  $\text{Na}_2\text{HPO}_4 \times 12\text{H}_2\text{O}$  (JSC Vekton, St. Petersburg, Russia);  $\text{K}_4[\text{Fe}(\text{CN})_6] \times 3\text{H}_2\text{O}$  (JSC Kupavnareaktiv, Staraya Kupavna, Russia);  $\text{KH}_2\text{PO}_4$  (NevaReaktiv Ltd., St. Petersburg, Russia); NaCl (OJSC Mikhailovsky Chemical Reagents Plant, Barnaul, Russia);  $\text{Na}_3\text{C}_6\text{H}_5\text{O}_7 \times 5.5\text{H}_2\text{O}$  (JSC ECOS-1, Moscow, Russia). These reagents were chemically pure. Other chemicals were 0.05 M  $\text{HAuCl}_4$  solution (RPE Tomanalyt Ltd., Tomsk, Russia); L-ascorbic acid BioXtra  $\geq 99\%$ , uric acid BioXtra  $\geq 99\%$ , L-glutathione reduced  $\geq 98\%$  (Sigma-Aldrich Co., St. Louis, MO, USA). Deionized water with a resistivity of  $18 \text{ M}\Omega \times \text{cm}$  was used as dissolvent.

### 2.2. Materials

A polymer film based on polyethylene terephthalate (PET), 0.25 mm thick (Fellowes Inc., Itasca, IL, USA) was used as a substrate for FFEs fabrication. CV based on polyacrylonitrile (M-Carbo Ltd., Minsk, Belarus) was used in the preparation of the indicator FFE. CV specifications are given in Table S1 of the Supplementary Materials. Silver conductive paint Mechanic DJ912 (Shenzhen Welsolo Electronic Technology Co., Ltd., Guangdong, China) was used in the preparation of the reference FFE. Cementit Universal (Merz + Benteli AG, Niederwangen, Switzerland) was used as an insulator. Microporous film MFAS-OS-2 based on cellulose acetate (CJSC STC Vladipor, Vladimir, Russia) was used as a membrane for  $[\text{Fe}(\text{CN})_6]^{3-/4-}$ . Five Russian-made phytocosmetic products were studied in the present work: cream-mousse, cream-gel, serum, day cream, and nourishing night cream. Their specifications are shown in Table S2 of the Supplementary Materials.

### 2.3. Apparatus

The LM-260iD laminator (Rayson Electrical MFG., Ltd., Guangdong, China) was used for single-sided hot lamination. The SPR-10 manual printer (DDM Novastar Inc., Ivyland, PA, USA) was used for screen printing. The IVA-5 inversion voltammetric analyzer (IVA Ltd., Yekaterinburg, Russia) was used for the potentiostatic electrodeposition of a precipitate containing a mixture of silver chloride and silver ferricyanide (SCSF). Two portable PA-S potentiometric analyzers (Ural State University of Economics, Yekaterinburg, Russia) were used for potentiometric measurements. A focused ion beam scanning electron microscope Auriga CrossBeam (Carl Zeiss NTS GmbH, Oberkochen, Germany) and Ultim

Max detector (Oxford Instruments plc., Abingdon, UK) were used for scanning electron microscopy (SEM) and energy-dispersive X-ray spectroscopy (EDS), respectively. An ultrasonic liquid processor VCX 750 (Sonics & Materials Inc., Newtown, CT, USA) with a stepped microtip ( $\varnothing$  2 mm) was used to produce emulsions. A digital multimeter Owon B41T+ (Fujian Lilliput Optoelectronics Technology Co., Ltd., Zhangzhou, China) with a thermocouple was used for the temperature control of emulsions. A pediatric sphygmomanometer LD-80 (Little Doctor Int. (S) Pte. Ltd., Yishun, Singapore) with 18–26 cm cuffs was used to fix the sensor system on the selected skin area. Installation Akvalab-UVOI-MF-1812 (JSC RPC Mediana Filter, Moscow, Russia) was used to obtain deionized water with a resistivity of  $18 \text{ M}\Omega \times \text{cm}$ .

#### 2.4. FFEs Manufacturing

FFEs were prepared by applying scalable technologies [43]. The indicator FFE was prepared by applying the single-sided hot lamination technology described in [41,42] and in the Supplementary Materials. The manufactured electrode was marked CV/PET and was used as the indicator FFE of the potentiometric sensor system. The size of one CV/PET was  $3 \times 35 \text{ mm}$ . The CV/PET was modified with gold nanoparticles (AuNPs) in order to improve its potential stability. The procedure of AuNPs synthesis and the technique of electrode modification are identical to those described in [30].

The reference FFE was manufactured on the basis of PET and silver paint using the screen-printing method, with the subsequent electrodeposition of a SCSF in the potentiostatic mode. The applied silver paint was oven-dried at  $110 \text{ }^\circ\text{C}$  for 30 min. The silver electrodes were cooled to room temperature and then cut to the required dimension  $3 \times 35 \text{ mm}$ . The middle part of the silver electrodes, which separated the working and contact zones, was covered with a mixture of insulator and acetone in a ratio of 1 to 5 by volume. The geometric area of the working area of one electrode was  $6\text{--}9 \text{ mm}^2$  ( $3 \times 2\text{--}3 \text{ mm}$ ). Modification of the silver electrode included the electrodeposition of a SCSF on the working surface, according to the technique described in [44]. For that purpose, the silver electrode was inserted in a continuously stirred buffer solution pH 5 (see Table S3 in Supplementary Materials) that contained  $1 \text{ mM K}_3[\text{Fe}(\text{CN})_6]$  and  $0.05 \text{ mM K}_4[\text{Fe}(\text{CN})_6]$ , and then, it was polarized at a constant potential of  $0.325 \text{ V}$  (vs. Ag/AgCl/KCl, 3.5 M) for 120 s. The resulting electrode was labeled SCSF/Ag/PET and used as a reference FFE in a potentiometric sensor system.

#### 2.5. CHPM Implementation

##### 2.5.1. Assembly of the Potentiometric Sensor System

The standard two-electrode configuration of the potentiometric sensor system includes one indicator electrode and one reference electrode, which are in contact with a membrane containing  $[\text{Fe}(\text{CN})_6]^{3-/4-}$  [29]. In this study, prior to measurements, the membrane was kept in a buffer solution pH 5 (see Table S3 in Supplementary Materials) containing  $1 \text{ mM K}_3[\text{Fe}(\text{CN})_6]$  and  $0.05 \text{ mM K}_4[\text{Fe}(\text{CN})_6]$  for 3–5 min. The choice of the solution composition is due to the fact that it has sufficient electrical conductivity and its pH corresponds to the physiological pH value of healthy human skin [45]. An increase in the number of indicator electrodes in the potentiometric sensor system led to a change in its electrode configuration. The three-electrode configuration of the potentiometric sensor system was first proposed to determine the AOA of human skin in [30]. Figure 1a illustrates the relevant process. This three-electrode configuration where  $E_1 = E_3 =$  indicator electrodes (in our work, it is CV/PET) and  $E_2 =$  reference electrode (in our work, it is SCSF/Ag/PET), allows us to obtain two results simultaneously and correctly evaluate the reproducibility of the measurement. This approach is important, since the human skin is a complex analytical object and its parameters, including AOA, may change over time affected by various external and internal factors. To minimize the impact of a variable skin condition on the results, the time interval between repeated measurements should tend to zero. The use of a three-electrode configuration of a potentiometric sensor system meets this condition,

since two results can be obtained during one measurement. In the present study, all components of the sensor system were flexible (Figure 1b); hence, it was called the “flexible potentiometric sensor system” (FPSS).

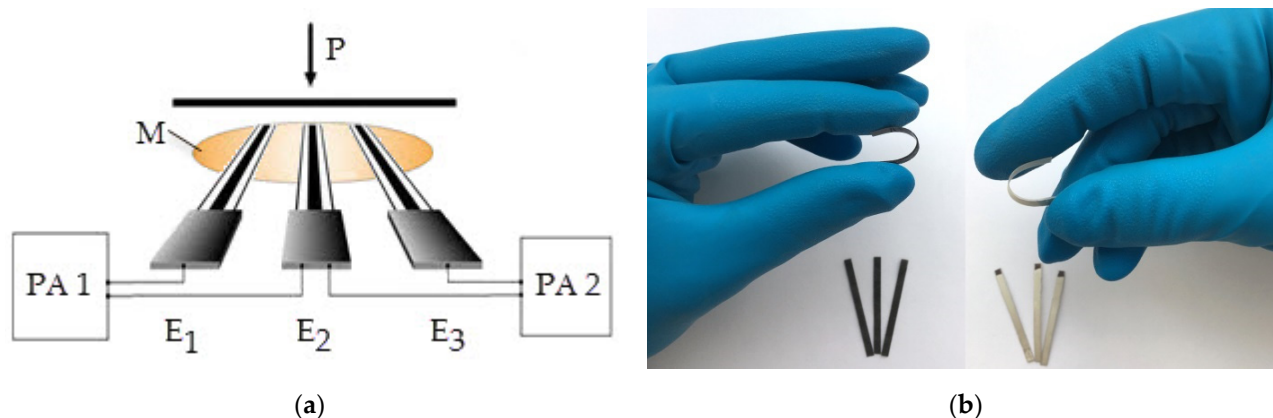


**Figure 1.** The circuit for performing measurement using a three-electrode configuration potentiometric sensor system ( $E_1$ ,  $E_2$ , and  $E_3$ : electrodes; M: membrane with  $[\text{Fe}(\text{CN})_6]^{3-/4-}$ ; PA 1 and PA 2: potentiometric analyzers; P: load) (a) and the pictures of fabricated flexible film electrodes (FFEs): carbon veil (CV)/polyethylene terephthalate (PET) (left) and silver chloride and silver ferricyanide (SCSF)/Ag/PET (right) (b).

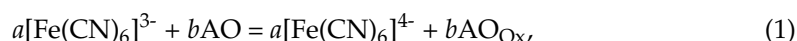
### 2.5.2. Model Conditions

In the model conditions, the membrane containing  $[\text{Fe}(\text{CN})_6]^{3-/4-}$  was placed on the table surface atop an inert (fluoroplastic) film. FFEs were applied to the membrane. Then, a steel 0.5 kg weight (base diameter = 36 mm) was set on top. The pressure exerted on the FPSS was approximately 4.82 kPa or 36.1 mm Hg.

### 2.5.3. Determining the AOA of Volunteers' Skin

Six young non-smoking women aged 24–28, with skin phototype II–III (hereinafter referred to as volunteers) were involved in the present study. The skin phototype of each volunteer was determined using the Fitzpatrick scale as described in [46,47]. Five volunteers participated in the skin AOA analysis in order to determine analytical characteristics of the developed FPSS. One volunteer was involved in evaluating the effectiveness of commercially available phytocosmetic products. The exclusion criteria were malnutrition, the intake of dietary supplements 7 days before the start of the measurements, and the use of cosmetic products other than those provided for the present experiment on the day of the analysis.

The three-electrode FPSS configuration was attached to the selected area of the skin (inside hand from the palm to the elbow) in such a way that the impregnated  $[\text{Fe}(\text{CN})_6]^{3-/4-}$  membrane was in contact with the skin surface, and FFEs were in contact with the membrane. The FPSS was fixed on the selected area of the arm with the help of a sphygmomanometer cuff, which was inflated to low pressure (35–40 mm Hg). This pressure was maintained during the entire measurement (10 min). Skin antioxidants diffused to the membrane, where they interacted with the oxidized form of the mediator by reaction (1):



where  $[\text{Fe}(\text{CN})_6]^{3-}$ —the oxidized form of the mediator; AO—antioxidant(s);  $[\text{Fe}(\text{CN})_6]^{4-}$ —the reduced form of the mediator;  $\text{AO}_{\text{Ox}}$ —the oxidized form of antioxidant(s);  $a$  and  $b$ —stoichiometric coefficients. The change in the ratio of the oxidized and reduced forms of the mediator in the membrane as a result of reaction (1) caused changes in the potential of the

indicator electrode and served as an analytical signal. The skin AOA (in mol-eq L<sup>-1</sup> = M-eq) was calculated by Formula (2):

$$AOA = \frac{C_{Ox} - aC_{Red}}{1 + a}, a = \left( \frac{C_{Ox}}{C_{Red}} \right) \cdot 10^{\left( \frac{\Delta E F}{2.3RT} \right)}, \quad (2)$$

where  $C_{Ox}$  and  $C_{Red}$  (in mol L<sup>-1</sup> = M)—respective concentrations of K<sub>3</sub>[Fe(CN)<sub>6</sub>] and K<sub>4</sub>[Fe(CN)<sub>6</sub>] in the membrane;  $\Delta E = E_2 - E_1$ —the change in the potential of the indicator electrode for 10 min from the initial ( $E_1$ , V) to the final ( $E_2$ , V) value;  $F = 96485.332$  C mol<sup>-1</sup>—the Faraday constant;  $R = 8.314$  J K<sup>-1</sup> mol<sup>-1</sup>—absolute gas constant;  $T$  (in K) =  $T$  (in °C) + 273.15—absolute temperature.

## 2.6. Analysis of Phytocosmetic Products

The effectiveness of phytocosmetic products (see Table S2 in Supplementary Materials) was measured in vitro and in vivo assays, applying the hybrid potentiometric method and CHPM respectively (see Table S6 in Supplementary Materials).

In vitro, AOA of phytocosmetic products was determined by the method described in [27] with some modifications. A sample of the phytocosmetic product was mixed with a pH 5 buffer solution containing 1 mM K<sub>3</sub>[Fe(CN)<sub>6</sub>] and 0.01 mM K<sub>4</sub>[Fe(CN)<sub>6</sub>] by ultrasound (frequency 20 kHz; amplitude 250 μmat; efficiency 20%) for 2 min. As a result, emulsions were obtained. The formation of emulsions by ultrasound was accompanied by their heating. The heated emulsions were cooled in a water bath to 25 ± 1 °C. The temperature was monitored by using a thermocouple of a multimeter lowered in the tube containing the emulsion. The emulsion AOA was expressed per 1 g of the initial phytocosmetic product according to Formula (3):

$$AOA = \frac{C_{Ox} - aC_{Red}}{1 + a} \cdot \frac{V}{m}, \quad (3)$$

where  $V$  (in L)—the volume of the obtained emulsion;  $m$  (in g)—the weight of the analyzed sample of a phytocosmetic product.

In vivo, the skin AOA was measured without applying (control) and after applying the phytocosmetic product. A three-electrode configuration of FPSS was used for measurements, and the computation of the skin AOA was completed applying Formula (2). The effectiveness of the analyzed phytocosmetics product was estimated as the deviation of the skin AOA on the area with the applied phytocosmetic product relative to the control area by Formula (4):

$$\Delta AOA = AOA_{(skin+phyto\ cosmetics)} - AOA_{skin}, \quad (4)$$

where  $AOA_{(skin+phytocosmetics)}$ —AOA of volunteer's skin with an applied phytocosmetic product;  $AOA_{skin}$ —AOA of volunteer's skin without a phytocosmetic product (control).

## 2.7. Statistical Analysis

The measurements were performed in 2–6-fold replication (4–6 times in the model conditions and 2 times on the human skin). Statistical analysis was performed in Microsoft Excel 2010 with an accepted significance level of 0.05. The data are presented as  $X \pm \Delta X$ , where  $X$  is the mean value and  $\Delta X$  is standard deviation. FPSS validation was performed by the spike recovery test with the use of non-enzymatic antioxidants present in the human skin. The recovery of non-enzymatic antioxidants was determined in accordance with IUPAC recommendations [48]. The relative standard deviation was used to determine the reproducibility of the measurement results. The correlation analysis was performed by calculating the Pearson correlation coefficient.

### 3. Results and Discussion

#### 3.1. FFEs Study

Measuring circuit in the Figure 1a, where  $E_1 = E_2 = E_3 = \text{CV/PET}$  or  $\text{AuNPs/CV/PET}$  or  $\text{SCSF/Ag/PET}$ , was used to study the stability of the FFEs under the model conditions. The results are presented in Table 1.

**Table 1.** Studies of FFEs stability under model conditions (n = 6).

FFE	$\tau^1$ , s	E <sup>2</sup> , mV	$E_{\max}-E_{\min}$ <sup>3</sup> , mV
CV/PET	250 ± 50	1 ± 0	2
AuNPs/CV/PET	317 ± 93	3 ± 2	6
SCSF/Ag/PET	233 ± 58	1 ± 1	1

<sup>1</sup>  $\tau$ : potential stabilization time. <sup>2</sup> E: stable potential value. <sup>3</sup>  $E_{\max}-E_{\min}$ : range of potential variation.

The time of establishing the potentials of all studied FFEs is less than the duration of measuring skin AOA (10 min or 600 s). However, the CV/PET has a potential of better reproducibility and a shorter period of its stabilization as compared with the electrode modified with gold nanoparticles (AuNPs/CV/PET). Unlike the carbon screen-printed electrode with a flat surface, whose modification with gold nanoparticles led to its better stability [30], the CV/PET surface is three-dimensional and consists of randomly coupled carbon fibers with a diameter of 5–10  $\mu\text{m}$  and an unevenly distributed polyester binder (see Figure S1 in Supplementary Materials and [41,42]). The three-dimensional structure of the CV/PET excludes the formation of a surface flat layer containing AuNPs, since AuNPs penetrate through pores into the inner layers of the CV. This results in a mixed potential detecting AuNPs and CV simultaneously. Due to the registration of a mixed potential, the AuNPs/CV/PET demonstrates a worse potential stability than the CV/PET. The characteristics of the electrode that differ from the SCSF/Ag/PET by the non-conductive substrate (alumina ceramics), by SEM, were described in [44]. It was shown that small  $\text{Ag}_3[\text{Fe}(\text{CN})_6]$  crystals fill the pores between large AgCl crystals, which leads to a greater stability of the potential of the electrode with a mixed precipitate ( $\text{Ag}_3[\text{Fe}(\text{CN})_6] + \text{AgCl}$ ) as compared with a silver chloride electrode (AgCl only) in a medium (solution, membrane) containing  $[\text{Fe}(\text{CN})_6]^{3-/4-}$ . Since the non-electrically conductive substrate does not affect the potentiostatic electrodeposition of the precipitate, the results presented in [44] are fully valid for the SCSF/Ag/PET. In further studies, the CV/PET and SCSF/Ag/PET were used as the indicator and the reference electrodes of the FPSS, respectively.

#### 3.2. FPSS Testing in Model Conditions

The three-electrode configuration of the FPSS ( $E_1 = E_3 = \text{CV/PET}$  and  $E_2 = \text{SCSF/Ag/PET}$  in Figure 1a) was tested under the model conditions to confirm its analytical effectiveness. Figure 2 illustrates the dependence of the FPSS potential on the logarithm of the concentration ratio of the oxidized and reduced forms of the mediator in the membrane, which is linear with an approximation coefficient  $R^2 > 0.99$ . The slope of this dependence is approximately 55 mV, which is in good agreement with the pre-logarithmic coefficient in the Nernst equation for a single-electron process, which is equal to 59 mV at 25 °C [49].

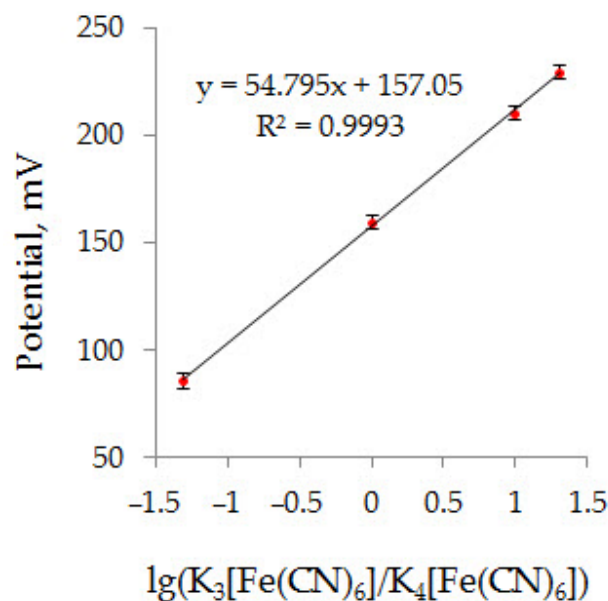


**Figure 2.** Dependence of the FPSS potential on the logarithm of  $K_3[Fe(CN)_6]/K_4[Fe(CN)_6]$  concentration ratio under model conditions ( $n = 4$ ).

The content of the non-enzymatic antioxidants in the human skin decrease in the following sequence: ascorbic acid > uric acid > reduced glutathione >  $\alpha$ -tocopherol > ubiquinol 10 [11]. Due to normal aging and photoaging, the content of ascorbic acid, reduced glutathione, and  $\alpha$ -tocopherol decreases, while the level of uric acid is relatively stable [12]. The non-enzymatic antioxidants prevailing in the human skin (ascorbic acid, uric acid, and reduced glutathione) were used to validate the measurement procedure. The results are presented in Table 2 and Table S4 of the Supplementary Materials. The results obtained for ascorbic acid are characterized by good analytical characteristics: reproducible (RSD) does not exceed 5.5%, and the recovery is close to 100% in the range of AOA 15–990  $\mu$ M-eq (see Table S4 of Supplementary Materials).

**Table 2.** Results of determining antioxidants and their mixtures with the use of FPSS under model conditions ( $n = 4$ ).

Model Solution	Expected AOA, $\mu$ M-eq	Measured AOA, $\mu$ M-eq	RSD, %	Recovery, %	$t^1$
L-ascorbic Acid (25 $\mu$ M)	50.0	49.0 $\pm$ 0.7	1.5	98 $\pm$ 1	2.51
Uric Acid (25 $\mu$ M)	50.0	48.9 $\pm$ 0.8	1.5	98 $\pm$ 1	2.76
L-glutathione Reduced (50 $\mu$ M)	50.0	51.0 $\pm$ 1.2	2.4	102 $\pm$ 2	1.64
L-ascorbic Acid (25 $\mu$ M) + Uric Acid (25 $\mu$ M)	100.0	91.8 $\pm$ 2.9	3.2	92 $\pm$ 3	5.63
L-ascorbic Acid (25 $\mu$ M) + L-glutathione Reduced (50 $\mu$ M)	100.0	101.0 $\pm$ 1.6	1.6	101 $\pm$ 2	1.21
L-ascorbic Acid (25 $\mu$ M) + Uric Acid (25 $\mu$ M) + L-glutathione Reduced (50 $\mu$ M)	150.0	144.8 $\pm$ 2.9	2.0	96 $\pm$ 2	3.61

<sup>1</sup> Student's  $t$  test:  $t_{\text{theor.}} = 3.18$  for  $f = n - 1 = 3$  and  $\alpha = 0.05$ .

There are no statistically significant differences between the expected and measured AOA values for individual antioxidants and the binary mixture of ascorbic acid and reduced glutathione (Table 2). The model solutions, including both ascorbic and uric acids showed a slight, but still statistically significant, decrease in the measured AOA as compared to the expected value. Apparently, this is due to the insignificant (typical for this degree of concentration) antagonism of these antioxidants. An antagonistic effect of mixtures of ascorbic and uric acids was also recorded for conventional spectrophotometric ORAC and ABTS assays and was related to the formation of adducts between these

antioxidants [50]. In general, biological objects are characterized by additive, synergistic, and antagonistic antioxidant effects [51]; that is why when characterizing the antioxidant status of a biological sample, preference should be given to the integral value due to its greater informativeness compared with the additive value.

### 3.3. Measuring AOA of Volunteers' Skin

Table 3 presents the results of determining the AOA of five volunteers' skin using a three-electrode FPSS configuration ( $E_1 = E_3 = \text{CV/PET}$  and  $E_2 = \text{SCSF/Ag/PET}$  in Figure 1a). RSD does not exceed 7.5%, and the values of the recovery of the model antioxidant (L-ascorbic acid), introduced into the membrane, indicate the absence of significant matrix effects.

**Table 3.** Results of determining antioxidant activity (AOA) of volunteers' skin and L-ascorbic acid additives with the use of FPSS (n = 2).

Volunteer No	AOA of Skin, $\mu\text{M-eq}$	RSD, %	Added L-Ascorbic Acid, $\mu\text{M-eq}$	Total AOA, $\mu\text{M-eq}$	Recovery, %
1	19.4 $\pm$ 1.4	7.5	50.0	70.8 $\pm$ 2.4	103 $\pm$ 2
2	26.1 $\pm$ 1.9	7.3	50.0	75.7 $\pm$ 4.1	99 $\pm$ 4
3	35.5 $\pm$ 2.3	6.4	50.0	85.8 $\pm$ 3.2	98 $\pm$ 2
4	41.0 $\pm$ 2.2	5.3	50.0	89.9 $\pm$ 3.5	98 $\pm$ 2
5	68.5 $\pm$ 3.1	4.6	50.0	118.3 $\pm$ 4.5	99 $\pm$ 3

### 3.4. Analysis of Phytocosmetic Products

The results of determining AOA of a volunteer's skin (a young woman) in the areas without application (control) and after application of the analyzed phytocosmetic product are given in Figures 3 and 4. The time of data collection equal to the duration of exposure of phytocosmetic products on the volunteer's skin was selected as a length of an average working day. All the analyzed phytocosmetic products demonstrated their effectiveness both in vitro (see Table S5 in Supplementary Materials) and in vivo assays (Figures 3 and 4).

Figure 4 presents the  $\Delta\text{AOA} = f(t)$  dependences which show how, after the application of phytocosmetic products, AOA of the volunteer's skin was changing for 8 h. The evidence of the antioxidant effect of the phytocosmetic product (t) was mounting in the following order: cream-mousse  $\approx$  cream-gel  $\approx$  serum ( $t \leq 5$  h) < day cream ( $t \leq 8$  h) < nourishing night cream ( $t > 8$  h). We have identified two types of  $\Delta\text{AOA} = f(t)$  dependencies. Cream-mousse, cream-gel, and serum demonstrated the first type of  $\Delta\text{AOA} = f(t)$  dependence (Figure 4a), while day cream and nourishing night cream demonstrated the second type of  $\Delta\text{AOA} = f(t)$  dependence (Figure 4b). We believe that the phytocosmetic products of the first type can be attributed to the express care category, and phytocosmetic products of the second type can be attributed to the cosmetics with the prolonged action. In this paper, we will limit ourselves with just this assumption and leave the further interpretation of the results to cosmetic chemists.

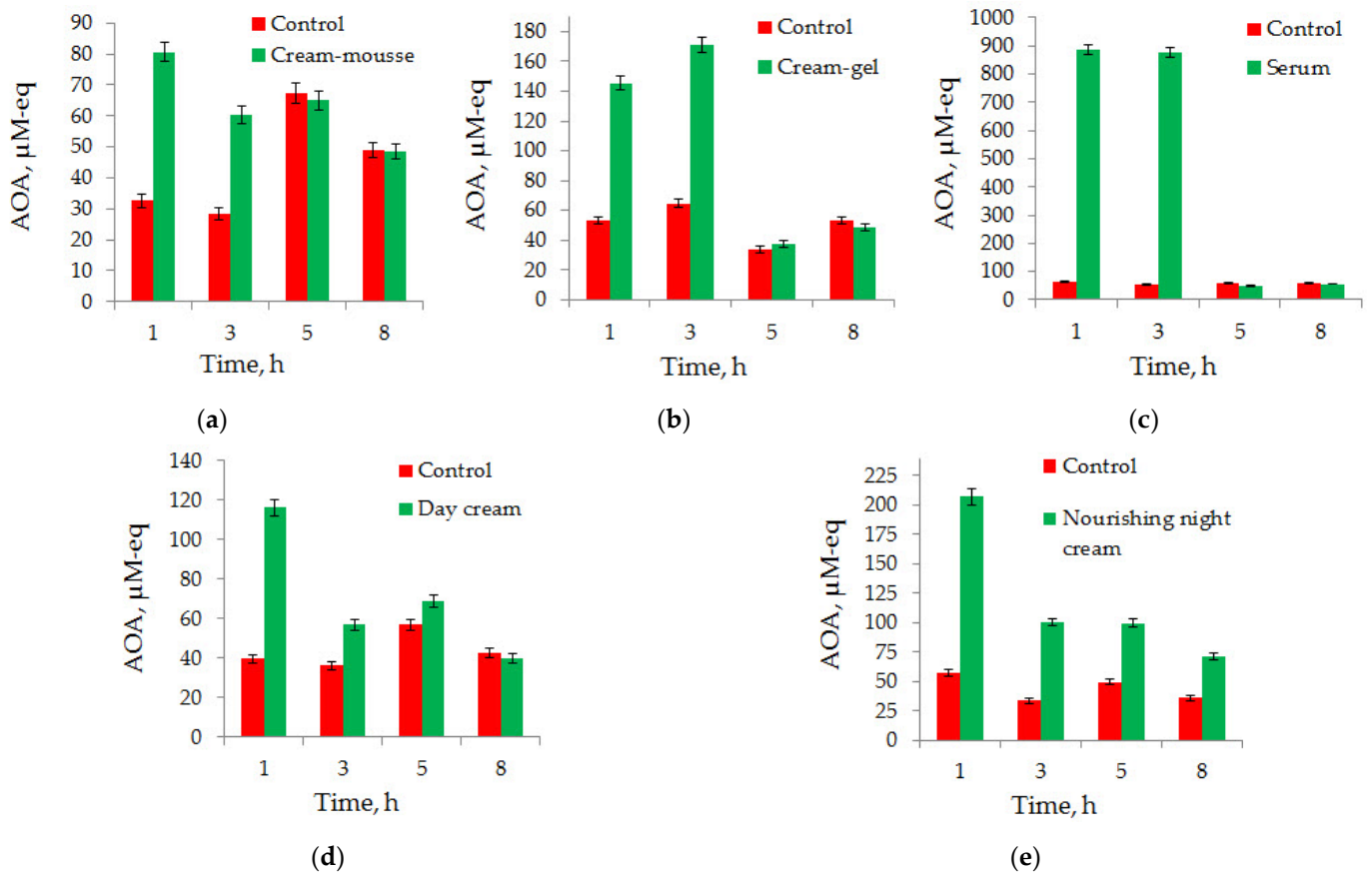


**Figure 3.** The results of measuring AOA of the volunteer’s skin with the use of three-electrode configuration of FPSS ( $n = 2$ ) on the areas without application (control) and after application of a phytocosmetic product: cream-mousse (a), cream-gel (b), serum (c), day cream (d), nourishing night cream (e). Time of exposition is expressed in hours.

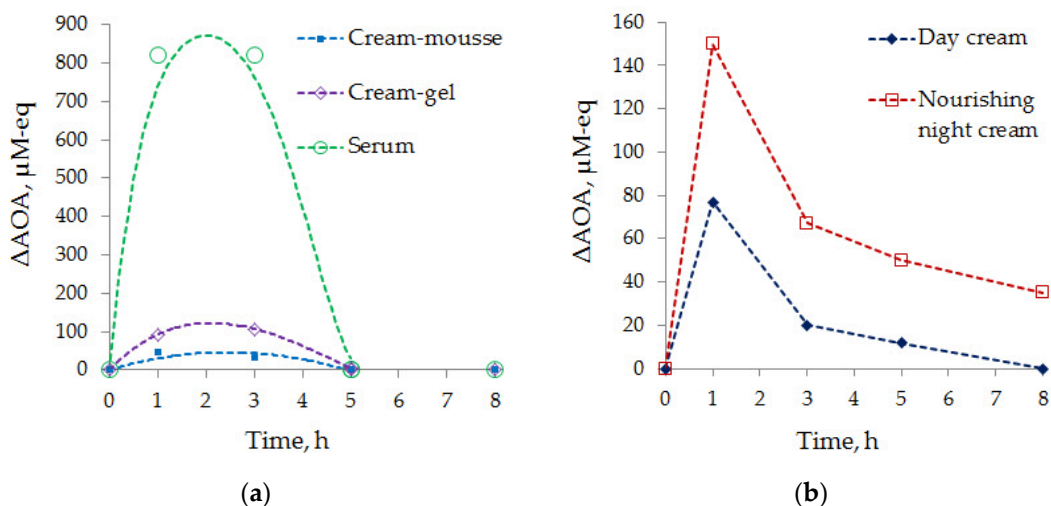


**Figure 4.** Effectiveness of phytocosmetic products presented as  $\Delta\text{AOA} = f(t)$  dependences for cream-mousse, cream-gel, serum (a); and day cream, nourishing night cream (b). Time of exposition is expressed in hours.

The AOA of the phytocosmetic product in vitro was correlated with its in vivo effectiveness. The Pearson correlation coefficient between the AOA of the phytocosmetic product obtained in an in vitro assay and the maximum effectiveness of the phytocosmetic product in vivo is equal to  $r = 0.92$  ( $p < 0.05$ ). These data are presented in Figure 5 and indicate that phytocosmetic products with higher AOA are able to ensure a higher antioxidant

status of the human skin. It is worth noting that the use of in vivo assay is preferable, since it most closely resembles the operating conditions of phytocosmetic products and therefore has a better reliability of the obtained results. In addition, in vivo assay enables evaluation of how long the effectiveness of the phytocosmetic product on the human skin can last (the duration of the antioxidant effect).

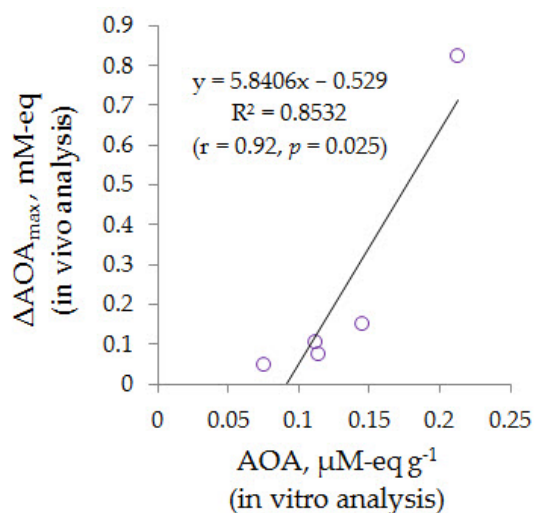


**Figure 5.** Correlation between AOA of phytocosmetic product (in vitro analysis) and  $\Delta\text{AOA}_{\text{max}}$  value of the phytocosmetic product (in vivo analysis).  $R^2$ : approximation reliability value;  $r$ : Pearson's correlation coefficient;  $p$ : significance level.

### 3.5. Comparison of the Obtained Findings with Earlier Studies

Brainina et al. [29] first proposed a membrane based on cellulose acetate as a mediator carrier  $[\text{Fe}(\text{CN})_6]^{3-/4-}$ , which, complete with commercially available electrodes, was used to determine the AOA of human skin. A shortcoming of this technique was a multiple use of the indicator platinum screen-printed electrode and the need for its sterilization (when the test volunteer changed) and regeneration (after a series of measurements). In their later work, Brainina et al. [30] proposed a disposable sensor system. Its effectiveness was exemplified with the biologically active food supplement Askorutin. However, the obtained findings showed a decrease in reproducibility as compared with the results received in [29]. In the present work, a disposable FPSS is proposed, and its effectiveness is exemplified with commercially available phytocosmetic products. The comparative results of these three potentiometric sensor systems are presented in Table 4, and it is apparent that the proposed FPSS enables obtaining the most reproducible results.

**Table 4.** Comparative characteristics of potentiometric sensor systems for non-invasive measurement of human skin AOA.

Electrodes		Mediator, mM		Range of AOA, $\mu\text{M-eq}$	RSD, %	Source
Indicator <sup>1</sup>	Reference <sup>2</sup>	$\text{K}_3[\text{Fe}(\text{CN})_6]$	$\text{K}_4[\text{Fe}(\text{CN})_6]$			
Pt/AC	H92SG	5	0	20–4000	$\leq 13$	[29]
AuNPs/C/FG	SCSF/Ag/FG	1	0.05	30–900 <sup>3</sup>	$\leq 20$	[30]
CV/PET	SCSF/Ag/PET	1	0.05	15–990 <sup>3</sup>	$\leq 7$	[This work]

<sup>1</sup> Pt/AC: commercial platinum screen-printed electrode on alumina ceramic; AuNPs/C/FG: carbon screen-printed electrode on fiberglass modified with gold nanoparticles; CV/PET: carbon veil electrode on polyethylene terephthalate. <sup>2</sup> H92SG: commercial ECG-type electrode; SCSF/Ag/FG: silver screen-printed electrode on fiberglass modified with silver chloride and silver ferricyanide; SCSF/Ag/PET: silver screen-printed electrode on polyethylene terephthalate modified with silver chloride and silver ferricyanide. <sup>3</sup> The range of determined values of skin AOA can be broadened if concentration of the mediator changes (see Table S6 in Supplementary Materials).

#### 4. Conclusions

The use of flexible, soft, and stretchable materials is the basis for creating tactile, including wearable, sensors that are advantageous in terms stability, reliability, and convenience as compared with conventional “rigid” electronic devices. The application of scalable technologies and the use of available materials contribute to the rapid prototyping of sensor devices. In this study, we have proposed a new disposable FPSS for non-invasive monitoring of the human skin AOA, which has been developed on the basis of low-cost materials with the use of scalable technologies. The FPSS has been tested in the model conditions and applied for determining the skin AOA of volunteers and for evaluating the impact of phytocosmetic products. Validation of the assay procedure has been performed using non-enzymatic antioxidants present in the human skin. The obtained results have shown good accuracy and reproducibility, which makes it possible to predict a broad applicability of the FPSS in real-time monitoring of the skin AOA as well as for evaluating the effectiveness of topically and orally applied antioxidants.

**Supplementary Materials:** The following are available online at <https://www.mdpi.com/article/10.3390/chemosensors9040076/s1>, Table S1: Specification of the carbon veil used in the study; Figure S1: SEM-images and EDS spectrum of CV/PET; Table S2: Characteristics of commercially available phytocosmetic products used in the study; Table S3: Composition of the buffer solution pH 5 used in the study; Table S4: Results of L-ascorbic acid determination using FPSS under model conditions (n = 4); Table S5: Effectiveness of commercially available phytocosmetic products; Table S6: The theoretical range of the AOA determined values.

**Author Contributions:** Conceptualization, N.Y.S. and A.V.T.; methodology, A.V.T.; validation, E.I.K. and M.A.B.; formal analysis, A.V.T.; investigation, E.I.K. and M.A.B.; resources, A.V.T.; writing—original draft preparation, A.V.T.; writing—review and editing, N.Y.S.; visualization, A.V.T.; supervision, A.V.T.; project administration, A.V.T. and N.Y.S. All authors have read and agreed to the published version of the manuscript.

**Funding:** This research received no external funding.

**Institutional Review Board Statement:** The study was conducted in accordance with the Declaration of Helsinki, and the protocol was approved by the Ethics Committee of JSC Medical Technologies (The Project Identification Code: 101-05/18).

**Informed Consent Statement:** Informed consent was obtained from all subjects involved in the study.

**Data Availability Statement:** The datasets used and/or analyzed during the current study are available from the corresponding author upon reasonable request.

**Acknowledgments:** The authors would like to thank M-Carbo Ltd. and personally A. Konovalchik, Chief Business Development Officer, for providing carbon veil used in the present study. The authors are also grateful to RPE Tomanalyt Ltd. and personally to G. Noskova, Deputy CEO, for manufacturing interconnect cables used to build a three-electrode configuration of the potentiometric sensor system.

**Conflicts of Interest:** The authors declare no conflict of interest.

#### References

1. Halliwell, B.; Gutteridge, J.M.C. The skin. In *Free Radicals in Biology and Medicine*, 5th ed.; Halliwell, B., Gutteridge, J.M.C., Eds.; Oxford University Press: Oxford, UK, 2015; Chapter 7.13; pp. 402–408.
2. Wölfle, U.; Seelinger, G.; Bauer, G.; Meinke, M.C.; Lademann, J.; Schempp, C.M. Reactive molecule species and antioxidative mechanisms in normal skin and skin aging. *Skin Pharmacol. Physiol.* **2014**, *27*, 316–332. [[CrossRef](#)] [[PubMed](#)]
3. Moldogazieva, N.T.; Mokhosev, I.M.; Feldman, N.B.; Lutsenko, S.V. ROS and RNS signalling: Adaptive redox switches through oxidative/nitrosative protein modifications. *Free Radic. Res.* **2018**, *52*, 507–543. [[CrossRef](#)] [[PubMed](#)]
4. Aseervatham, G.S.B.; Sivasudha, T.; Jeyadevi, R.; Ananth, D.A. Environmental factors and unhealthy lifestyle influence oxidative stress in humans—An overview. *Environ. Sci. Pollut. Res.* **2013**, *20*, 4356–4369. [[CrossRef](#)] [[PubMed](#)]
5. Rinnerthaler, M.; Bischof, J.; Streubel, M.K.; Trost, A.; Richter, K. Oxidative stress in aging human skin. *Biomolecules* **2015**, *5*, 545–589. [[CrossRef](#)]
6. Baek, J.; Lee, M.-G. Oxidative stress and antioxidant strategies in dermatology. *Redox Rep.* **2016**, *21*, 164–169. [[CrossRef](#)] [[PubMed](#)]

7. Anunciato, T.P.; da Rocha Filho, P.A. Carotenoids and polyphenols in nutricosmetics, nutraceuticals, and cosmeceuticals. *J. Cosmet. Dermatol.* **2012**, *11*, 51–54. [[CrossRef](#)] [[PubMed](#)]
8. Lall, N.; Mahomoodally, M.F.; Esposito, D.; Steenkamp, V.; Zengin, G.; Steyn, A.; Oosthuizen, C.B. Editorial: Cosmeceuticals from medicinal plants. *Front. Pharmacol.* **2020**, *11*, 1149. [[CrossRef](#)]
9. Brainina, K.; Stozhko, N.; Vidrevich, M. Antioxidants: Terminology, Methods, and Future Considerations. *Antioxidants* **2019**, *8*, 297. [[CrossRef](#)]
10. Portugal-Cohen, M.; Kohen, R. Non-invasive evaluation of skin cytokines secretion: An innovative complementary method for monitoring skin disorders. *Methods* **2013**, *61*, 63–68. [[CrossRef](#)]
11. Shindo, Y.; Witt, E.; Han, D.; Epstein, W.; Packer, L. Enzymic and non-enzymic antioxidants in epidermis and dermis of human skin. *J. Investig. Dermatol.* **1994**, *102*, 122–124. [[CrossRef](#)]
12. Rhie, G.; Shin, M.H.; Seo, J.Y.; Choi, W.W.; Cho, K.H.; Kim, K.H.; Park, K.C.; Eun, H.C.; Chung, J.H. Aging- and photoaging-dependent changes of enzymic and nonenzymic antioxidants in the epidermis and dermis of human skin in vivo. *J. Investig. Dermatol.* **2001**, *117*, 1212–1217. [[CrossRef](#)]
13. Dabbagh, A.J.; Frei, B. Human suction blister interstitial fluid prevents metal ion-dependent oxidation of low density lipoprotein by macrophages and in cell-free systems. *J. Clin. Investig.* **1995**, *96*, 1958–1966. [[CrossRef](#)] [[PubMed](#)]
14. Granger, C.; Aladren, S.; Delgado, J.; Garre, A.; Trullas, C.; Gilaberte, Y. Prospective evaluation of the efficacy of a food supplement in increasing photoprotection and improving selective markers related to skin photo-ageing. *Dermatol. Ther.* **2020**, *10*, 163–178. [[CrossRef](#)]
15. Ermakov, I.V.; Gellermann, W. Dermal carotenoid measurements via pressure mediated reflection spectroscopy. *J. Biophotonics* **2012**, *5*, 559–570. [[CrossRef](#)] [[PubMed](#)]
16. Ermakov, I.V.; Gellermann, W. Optical detection methods for carotenoids in human skin. *Arch. Biochem. Biophys.* **2015**, *572*, 101–111. [[CrossRef](#)] [[PubMed](#)]
17. Ermakov, I.V.; Ermakova, M.; Sharifzadeh, M.; Gorusupudi, A.; Farnsworth, K.; Bernstein, P.S.; Stookey, J.; Evans, J.; Arana, T.; Tao-Lew, L.; et al. Optical assessment of skin carotenoid status as a biomarker of vegetable and fruit intake. *Arch. Biochem. Biophys.* **2018**, *646*, 46–54. [[CrossRef](#)]
18. Ermakov, I.V.; Ermakova, M.R.; McClane, R.W.; Gellermann, W. Resonance Raman detection of carotenoid antioxidants in living human tissues. *Opt. Lett.* **2001**, *26*, 1179–1181. [[CrossRef](#)]
19. Haag, S.F.; Taskoparan, B.; Darwin, M.E.; Groth, N.; Lademann, J.; Sterry, W.; Meinke, M.C. Determination of the antioxidative capacity of the skin in vivo using resonance Raman and electron paramagnetic resonance spectroscopy. *Exp. Dermatol.* **2011**, *20*, 483–487. [[CrossRef](#)]
20. Fuchs, J.; Groth, N.; Herrling, T. In vivo measurement of oxidative stress status in human skin. *Methods Enzymol.* **2002**, *352*, 333–339. [[CrossRef](#)]
21. Lohan, S.B.; Lauer, A.-C.; Arndt, S.; Friedrich, A.; Tschersch, K.; Haag, S.F.; Darwin, M.E.; Vollert, H.; Kleemann, A.; Gersonde, I.; et al. Determination of the antioxidant status of the skin by in vivo-electron paramagnetic resonance (EPR) spectroscopy. *Cosmetics* **2015**, *2*, 286–301. [[CrossRef](#)]
22. Arbault, S.; Pebay, C.; Amatore, C.; Lachmann-Weber, N.; Heusele, C.; Renimel, I. Electrochemical Device and Method for Measuring the Redox State of the Skin. Patent WO2007077360-A1, 12 July 2007.
23. Ruffien-Ciszak, A.; Gros, P.; Comtat, M.; Schmitt, A.-M.; Questel, E.; Casas, C.; Redoules, D. Exploration of the global antioxidant capacity of the stratum corneum by cyclic voltammetry. *J. Pharm. Biomed. Anal.* **2006**, *40*, 162–167. [[CrossRef](#)] [[PubMed](#)]
24. Guitton, C.; Ruffien-Ciszak, A.; Gros, P.; Comtat, M. Voltammetric sensors for the determination of antioxidant properties in dermatology and cosmetics. In *Comprehensive Analytical Chemistry*; Alegret, S., Merkoçi, A., Eds.; Elsevier, B.V.: Amsterdam, The Netherlands, 2007; Volume 49, pp. 163–180. [[CrossRef](#)]
25. Kohen, R.; Fanberstein, D.; Zelkowitz, A.; Tirosh, O.; Farfour, S. Noninvasive in vivo evaluation of skin antioxidant activity and oxidation status. *Methods Enzymol.* **1999**, *300*, 428–437. [[CrossRef](#)] [[PubMed](#)]
26. Brainina, K.Z.; Galperin, L.G.; Gerasimova, E.L.; Khodos, M.Y. Noninvasive potentiometric method of determination of skin oxidant/antioxidant activity. *IEEE Sens. J.* **2012**, *12*, 527–532. [[CrossRef](#)]
27. Brainina, K.Z.; Gerasimova, E.L.; Varzakova, D.P.; Kazakov, Y.E.; Galperin, L.G. Noninvasive method of determining skin antioxidant/oxidant activity: Clinical and cosmetics applications. *Anal. Bioanal. Electrochem.* **2013**, *5*, 528–542.
28. Markina, M.; Lebedeva, E.; Neudachina, L.; Stozhko, N.; Brainina, K. Determination of antioxidants in human skin by capillary zone electrophoresis and potentiometry. *Anal. Lett.* **2016**, *49*, 1804–1815. [[CrossRef](#)]
29. Brainina, K.Z.; Markina, M.G.; Stozhko, N.Y. Optimized potentiometric assay for non-invasive investigation of skin antioxidant activity. *Electroanalysis* **2018**, *30*, 2405–2412. [[CrossRef](#)]
30. Brainina, K.; Tarasov, A.; Khamzina, E.; Kazakov, Y.; Stozhko, N. Disposable potentiometric sensory system for skin antioxidant activity evaluation. *Sensors* **2019**, *19*, 2586. [[CrossRef](#)]
31. Pisoschi, A.M.; Cimpeanu, C.; Predoi, G. Electrochemical methods for total antioxidant capacity and its main contributors determination: A review. *Open Chem.* **2015**, *13*, 824–856. [[CrossRef](#)]
32. Brainina, K.Z.; Tarasov, A.V.; Kazakov, Y.E.; Vidrevich, M.B. Platinum electrode regeneration and quality control method for chronopotentiometric and chronoamperometric determination of antioxidant activity of biological fluids. *J. Electroanal. Chem.* **2018**, *808*, 14–20. [[CrossRef](#)]

33. Heikenfeld, J.; Jajack, A.; Rogers, J.; Gutruf, P.; Tian, L.; Pan, T.; Li, R.; Khine, M.; Kim, J.; Wang, J.; et al. Wearable sensors: Modalities, challenges, and prospects. *Lab Chip* **2018**, *18*, 217–248. [CrossRef] [PubMed]
34. Piro, B.; Mattana, G.; Noël, V. Recent advances in skin chemical sensors. *Sensors* **2019**, *19*, 4376. [CrossRef] [PubMed]
35. Herbert, R.; Kim, J.-H.; Kim, Y.S.; Lee, H.M.; Yeo, W.-H. Soft material-enabled, flexible hybrid electronics for medicine, healthcare, and human-machine interfaces. *Materials* **2018**, *11*, 187. [CrossRef]
36. Chen, B.-H.; Chuang, S.-I.; Duh, J.-G. Convertibility of anode electrode with micro-sized wafer scraps via carbon veil with plasma technique. *ACS Sustain. Chem. Eng.* **2017**, *5*, 1784–1793. [CrossRef]
37. Shin, D.; Shen, C.; Sanghadasa, M.; Lin, L. Breathable 3D supercapacitors based on activated carbon fiber veil. *Adv. Mater. Technol.* **2018**, *3*, 1800209. [CrossRef]
38. Gajda, I.; You, J.; Santoro, C.; Greenman, J.; Ieropoulos, I.A. A new method for urine electrofiltration and long term power enhancement using surface modified anodes with activated carbon in ceramic microbial fuel cells. *Electrochim. Acta* **2020**, *353*, 136388. [CrossRef]
39. Honeychurch, K.C.; Hart, J.P. Determination of flunitrazepam and nitrazepam in beverage samples by liquid chromatography with dual electrode detection using a carbon fibre veil electrode. *J. Solid State Electrochem.* **2008**, *12*, 1317–1324. [CrossRef]
40. Liu, C.; Li, M.; Gu, Y.; Gong, Y.; Liang, J.; Wang, S.; Zhang, Z. Resistance heating forming process based on carbon fiber veil for continuous glass fiber reinforced polypropylene. *J. Reinf. Plast. Compos.* **2018**, *37*, 366–380. [CrossRef]
41. Brainina, K.Z.; Bukharinova, M.A.; Stozhko, N.Y.; Sokolov, S.V.; Tarasov, A.V.; Vidrevich, M.B. Electrochemical sensor based on a carbon veil modified by phytosynthesized gold nanoparticles for determination of ascorbic acid. *Sensors* **2020**, *20*, 1800. [CrossRef] [PubMed]
42. Stozhko, N.Y.; Bukharinova, M.A.; Khamzina, E.I.; Tarasov, A.V.; Sokolov, S.V. Film carbon veil-based electrode modified with Triton X-100 for nitrite determination. *Chemosensors* **2020**, *8*, 78. [CrossRef]
43. Gonzalez-Macia, L.; Killard, A.J. Screen printing and other scalable point of care (POC) biosensor processing technologies. In *Medical Biosensors for Point of Care (POC) Applications*; Narayan, R.J., Ed.; Elsevier: Amsterdam, The Netherlands, 2017; Chapter 4; pp. 69–98. [CrossRef]
44. Brainina, K.Z.; Tarasov, A.V.; Vidrevich, M.B. Silver chloride/ferricyanide-based quasi-reference electrode for potentiometric sensing applications. *Chemosensors* **2020**, *8*, 15. [CrossRef]
45. Proksch, E. pH in nature, humans and skin. *J. Dermatol.* **2018**, *45*, 1044–1052. [CrossRef] [PubMed]
46. D’Orazio, J.; Jarrett, S.; Amaro-Ortiz, A.; Scott, T. UV radiation and the skin. *Int. J. Mol. Sci.* **2013**, *14*, 12222–12248. [CrossRef] [PubMed]
47. Australian Radiation Protection and Nuclear Safety Agency. Fitzpatrick Skin Phototype. PDF. Available online: [https://www.arpana.gov.au/sites/default/files/legacy/pubs/RadiationProtection/FitzpatrickSkinType.pdf?acsf\\_files\\_redirect](https://www.arpana.gov.au/sites/default/files/legacy/pubs/RadiationProtection/FitzpatrickSkinType.pdf?acsf_files_redirect) (accessed on 19 January 2021).
48. Burns, D.T.; Danzer, K.; Townshend, A. Use of the term “recovery” and “apparent recovery” in analytical procedures (IUPAC Recommendations 2002). *Pure Appl. Chem.* **2002**, *74*, 2201–2205. [CrossRef]
49. Kahlert, H. Potentiometry. In *Electroanalytical Methods*, 2nd ed.; Scholz, F., Ed.; Springer: Berlin/Heidelberg, Germany, 2010; Chapter II.9; pp. 237–256. [CrossRef]
50. Błaż, A.; Pilaszek, T.; Grzelak, A.; Dragan, A.; Bartosz, G. Interaction between antioxidants in assays of total antioxidant capacity. *Food Chem. Toxicol.* **2008**, *46*, 2365–2368. [CrossRef]
51. Olszowy-Tomczyk, M. Synergistic, antagonistic and additive antioxidant effects in the binary mixtures. *Phytochem. Rev.* **2020**, *19*, 63–103. [CrossRef]